11. Koumoto, K.; Sakurai, K.; Shinkai, S.; Kunitake, T. *Polym. Prepr.* **2002**, *43*, 721.
12. Zhang, L.; Zhang, M.; Zhou, Q.; Chen, J.; Zeng, F. *Biosci. Biotechnol. Biochem.* **2000**, *64*, 2172.
13. Hatanaka, K.; Yoshida, T.; Uryu, T.; Yoshida, O.; Nakashima, H.; Yamamoto, N.; Mimura, T.; Kaneko, Y. *Jpn. J. Cancer Res.* **1989**, *80*, 95–98.
14. Kaneko, Y.; Yoshida, O.; Nagasawa, R.; Hatanaka, K.; Yoshida, Y.; Date, M.; Ogiwara, S.; Shioya, S.; Matsuzawa, Y.; Nagashima, N.; Irie, Y.; Mimura, T.; Shinkai, H.; Yasuda, N.; Matsuzaki, K.; Uryu, T.; Yamamoto, N. *Biochem. Pharmacol.* **1990**, *39*, 793–797.
15. Miyano, H.; Nakagawa, R.; Suzuki, E.; Uryu, T. *Carbohydr. Res.* **1992**, *235*, 29–39.
16. Yoshida, T.; Yasuda, Y.; Mimura, T.; Kaneko, Y.; Nakashima, H.; Yamamoto, N.; Uryu, T. *Carbohydr. Res.* **1995**, *276*, 425–436.
17. Koumoto, K.; Kimura, T.; Mizu, M.; Sakurai, K.; Shinkai, S. *Chem. Commun.* **2001**, 1962–1963.
18. Koumoto, K.; Kimura, T.; Mizu, M.; Kunitake, T.; Sakurai, K.; Shinkai, S. *J. Chem. Soc., Perkin Trans. 1* **2002**, 2477–2484.
19. Sakurai, K.; Iguchi, R.; Mizu, M.; Koumoto, K.; Shinkai, S. *Bioorg. Chem.* **2003**, *31*, 216–226.
20. Saenger, W. *Principles of Nucleic Acid Structure*; Springer: New York, 1984.
21. Koumoto, K.; Kimura, T.; Sakurai, K.; Shinkai, S. *Bioorg. Chem.* **2001**, *29*, 178–185.

Polymer Journal, Vol. 35, No. 9, pp 714—720 (2003)

Polysaccharide–Polynucleotide Complexes Part 17. Solvent Effects on Conformational-Transition of Polydeoxyadenylic Acid in the Complexes with Schizophyllan

Masami MIZU, Kazuya KOUMOTO, Taro KIMURA,*
Kazuo SAKURAI,† and Seiji SHINKAI**

Department of Chemical Process & Environments, The University of Kitakyushu, 1–1 Hibikino, Wakamatu-ku, Kitakyushu, Fukuoka 808–0135, Japan
**Biotechnology and Food Research Institute, Fukuoka Industrial Technology Center, 1465–5 Aikawa, Kurume, Fukuoka 839–0861, Japan*
***Faculty of Engineering Department of Chemistry & Biochemistry, Graduate School of Engineering, Kyushu University, 6–10–1 Hakozaki, Higashi-ku, Fukuoka, Fukuoka 812–8581, Japan*

(Received May 9, 2003; Accepted July 7, 2003)

ABSTRACT: This paper examines the relationship between the conformation and solvent for the poly(dA)/s-SPG complex using circular dichroism in the 240–300 nm wavelength region. At the low temperature and low salt concentration, poly(dA) in the complex is estimated to take *C2'-endo* with a different torsional angle from the *anti* form. With increasing temperature, the circular dichroism (CD) spectrum starts to bear characteristics of *C3'-endo* and *anti* as a minority among the majority of *C2'-endo* and *anti*. When the salt concentration is increased, the spectrum becomes almost identical to that of the high temperature form under the non-salt condition. Therefore, addition of salt provides the identical effect to increasing temperature. D_2O induces the same effect as decreasing temperature.

KEY WORDS Polysaccharide–Polynucleotide Complex / Thermodynamics / Solvent Effect / β-1,3-Glucan / Circular Dichroism / Polynucleotide /

Conformational changes in polynucleotides play important roles in biological systems.[1] A replication fork in DNA undergoes a conformational change when it interacts with a single-stranded polynucleotide binding protein (SSB).[2] This change disables the replication fork to retrieve hybridization, which is crucial to DNA replication. Powell and Gray[3] explored the conformational change induced by SSB, using poly(dA) as a model single-stranded DNA (ssDNA). Their circular dichroism (CD) data demonstrated that SSB induces the same conformational change in poly(dA) as that of heating poly(dA) or protonating the polymer at low pH. It seems that ssDNAs conformational response to external stimuli is one of the crucial issues to understand the relationship between ssDNA conformation and biological roles.[1,2]

Sakurai and Shinkai[4] are the first to demonstrate that a neutral β-1,3-glucan schizophyllan (SPG) can bind single homo-polynucleotides to change the conformation dramatically. Here, SPG is produced by *Schizophyllun commune* and belongs to the β-1,3-glucan family (Figure 1).[5] SPG exists in a triple helix in water and a single chain (s-SPG) in dimethyl sulfoxide (DMSO).[6,7] When a s-SPG/DMSO solution is diluted with water (renature), SPG can gain the triple helical conformation again.[8] When some polynucleotide

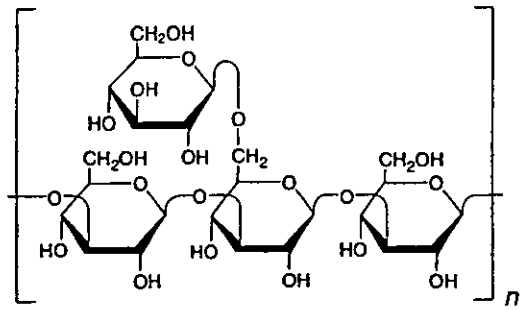

Figure 1. Chemical structure and repeating unit of schizophyllan.

is present in the renaturing process, a new triple helix consisting of one polynucleotide chain and two s-SPG chains is formed instead of reforming the original triple helix.[4] Mizu *et al.*[9] demonstrated that poly(dA) forms a complex with s-SPG and the complex exhibits the following features. (1) A critical base number is necessary to induce the complexation. (2) When the base number is > 60, the poly(dA) chain in the complex undergoes structural transition upon heating below the dissociation temperature (T_m) of the complex. This is a distinct conformational transition and we denote the low and higher temperature forms as HL and H, respectively. (3) The hypochromic effect once ceases at the transition temperature and appears again. Such complicated CD spectral changes have never been observed for single-stranded RNAs such as poly(C), poly(A), and

†To whom correspondence should be addressed.

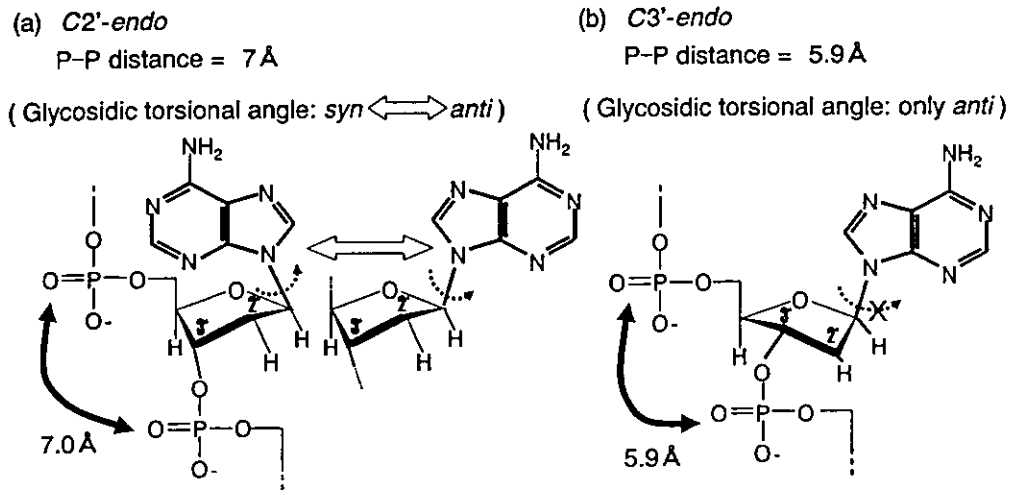

Figure 2. Schematic illustration of the conformational notation of polynucleotides. (a) *C2'-endo* puckering. For this puckering, the torsional angle of the glycosidic bond can be allowed to take two forms: *anti* and *syn*. The distance between the phosphate anions is 7.0 Å. (b) *C3'-endo* puckering. This puckering allows only *anti* form and the distance between the phosphate anions is 5.9 Å.

poly(U).[4,10] This spectral diversity is characteristic of poly(dA) and may be related to the conformational flexibility of DNA.[11] This paper examines the solvent effect of the complex made from poly(dA) and s-SPG to clarify the nature of this unique structural transition.

CONFORMATIONAL NOTATION OF POLYNUCLEOTIDES AND THE CD SPECTRUM FOR POLY(DA)

According to conformational studies on polynucleotides,[1,12] the ribose ring of ribonucleosides usually takes the *C3'-endo* puckering and the ribose in deoxyribonucleosides takes the *C2'-endo* puckering. Here, the *C3'-endo* puckering (or N-type) is a ribose puckering in which the *C3'* carbon is out-of-plane projecting out toward the same direction of the base moiety, and the *C2'-endo* puckering (or S-type) is defined in the same manner (see Figure 2). Torsional freedom around the glycosidic bond greatly differs between *C2'-endo* and *C3'-endo*. The *C3'-endo* puckering only takes the *anti* conformation which causes the Watson–Crick hydrogen-bonding sites to be directed far away from the ribose ring. The *C2'-endo* puckering enables the base to rotate rather freely and to take both *anti* and *syn* conformations. The *syn* form is an almost reverse position of the *anti* form, with Watson–Crick hydrogen-bonding sites now oriented towards the ribose. Generally, the *anti* form is more preferable than the *syn* form, however, the stability difference depends on the base molecules and the atmosphere surrounding the molecules. When the base is adenine, *anti* is more preferable than *syn*. The energy difference between those (*anti* and *syn*) is only 0.3 kcal mol^{-1},[12] small enough to convert each other. The electrostatic interaction between the phosphate anions plays an important role to determine the polynucleotide conformation, especially, the salt concentration dependence of the conformation. The distance between the adjacent phosphate anions is about 5.9 Å for the *C3'-endo* puckering, while 7.0 Å for the *C2'-endo* puckering.[1] Therefore, *C2'-endo* is more preferable in lower salt concentrations than *C3'-endo*, because electrostatic repulsion is less sealed in the lower salt concentration. The sugar puckering and the glycosidic bond angle are not defined as one conformation, but as a group of conformations having a similar steric parameter.[12] Polynucleotide chains contain *C2'-endo* and *C3'-endo* at the same time.

Circular dichroism in the 240–300 nm wavelength range reflects the spatial relationship between the adjacent bases along polynucleotides through the interactions between the induced dipole moment of the bases. Olsthoorn *et al.*[13,14] extensively studied the relationship between the CD spectra and the chain conformation of poly(dA) determined by NMR, and found that the poly(dA) chain consists of *C2'-endo* and *anti* (S_{dA}) as a major species and *C3'-endo* and *anti* (N_{dA}) as a minor one, and with increasing the chain length, the population of N_{dA} essentially vanishes.[15] Since the population of N_{dA}–N_{dA} should be negligible, only two combinations for the adjacent bases essentially determine the CD spectra, that is, S_{dA}–S_{dA} and S_{dA}–N_{dA} sequences. The CD spectra for S_{dA}–S_{dA} and S_{dA}–N_{dA} sequences are characterized to have a strong negative band at 250 nm and a weak positive band at 280 nm, and a strong negative band at 250 nm and a strong positive band at 260 nm, respectively.

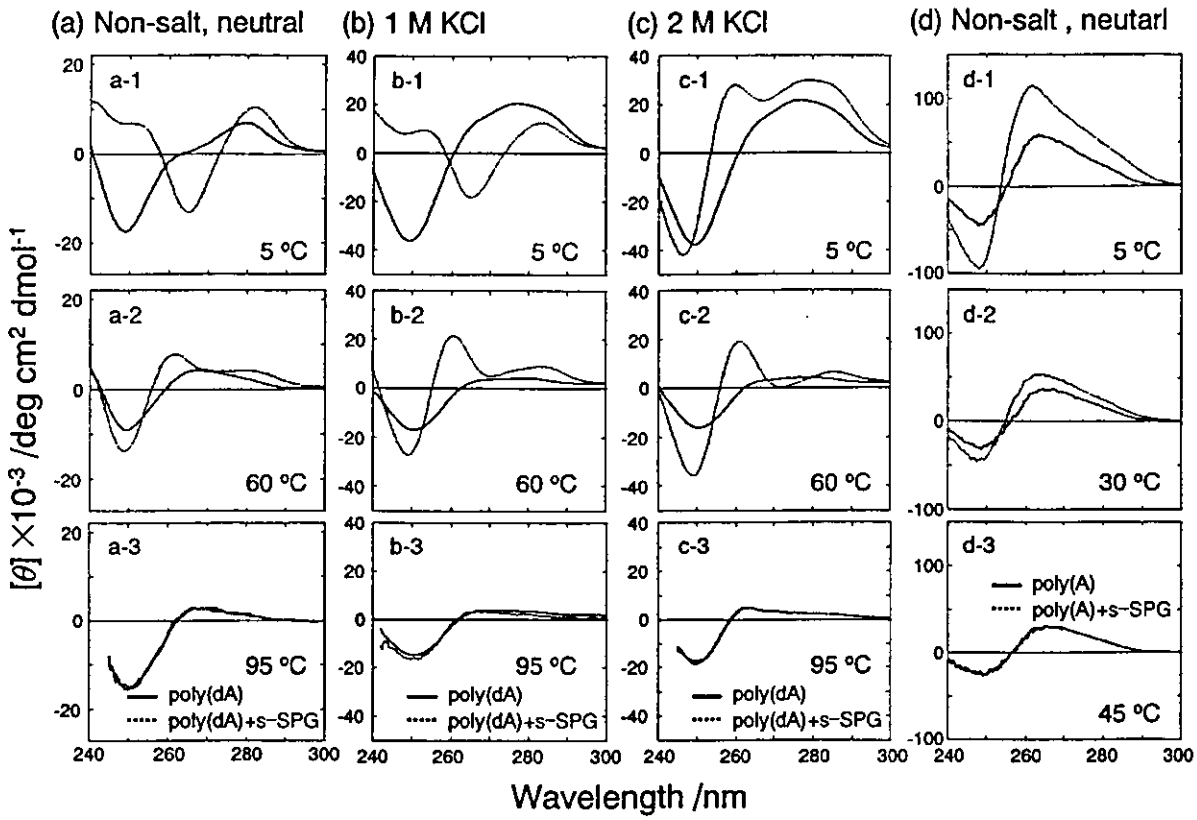

Figure 3. Comparison of the CD spectra in three solutions containing poly(dA) (non-salt and neutral: (a), 1 M KCl: (b), and 2 M KCl: (c)) at 5, 60, and 95 °C. For reference, poly(A) is shown in panel (d). In all panels, the solid and dotted lines represent the CD spectra for poly(dA) and the mixtures of poly(dA) and s-SPG.

EXPERIMENTAL

High-purity grades of NaCl, KCl, DMSO, D_2O, and formamide were purchased form Wako Chemical. Poly(dA) and poly(dT) were obtained from Amersham Phamacia and the degrees of polymerization, based on reported sedimentation velocities, were about 250 and 300, respectively. According to the previous work,[9] the poly(dA) base number of 250 was considered sufficient to ignore the chain end effect. The schizophyllan sample was kindly provided by Taito Co. in Japan. The molecular weight of s-SPG was 1.5×10^5, *i.e.*, 231 repeating units. A mixture of poly(dA) and s-SPG was prepared by adding a DMSO solution of s-SPG to an aqueous solution of poly(dA). Final concentrations of poly(dA) and s-SPG were 5.3×10^{-3} g dL^{-1} and 5.0×10^{-2} g dL^{-1}, respectively. The volume fraction of water in the mixture was 0.91 for all samples. Before measurements, all samples were annealed at 5 °C for 6–10 d. The CD and ultraviolet absorbance (UV) spectra in the 240–300 nm region were measured at 0–95 °C on a Jasco J-720WI spectropolarimeter and Jasco V-570 UV/VIS/NIR spectrophotometer, respectively. The CD and UV spectra depended only on the salt concentration, and the difference in cations did not provided any change. T_m was determined according to the established method.[4,9,10]

RESULTS AND DISCUSSION

Conformational Transition on Heating in Non-Salt and Neutral Solutions

Figure 3 presents the CD spectra in three solutions containing poly(dA) (non-salt and neutral: (a), 1 M KCl: (b), and 2 M KCl: (c)) at 5, 60, and 95 °C. For comparison, the poly(A) system is presented in panel (d). In all panels, the solid and dotted lines represent the CD spectra for poly(dA) and the mixtures of poly(dA) and s-SPG. Here, the mixture does not necessarily means the complex, but it may just consist of s-SPG and polynucleotide, individually. Hereinafter, we denote the complex and mixture as poly(dA)/s-SPG and poly(dA) + s-SPG, respectively. s-SPG is CD inactive at this wavelength, so that all change in CD should be ascribed to conformational changes in poly(dA).

In panel (a-1), there is considerable spectral difference between poly(dA) and poly(dA)/s-SPG. The spectrum of poly(dA) exhibits a typical feature for S_{dA}–S_{dA}, showing a strong negative band at 250 nm and a

weak positive band at 280 nm. Poly(dA)/s-SPG demonstrates an exciton-couple type band, showing a strong positive band at 283 nm and a new negative band at 265 nm. In the previous communication,[9] this spectrum was denoted as HL (see appendix) and, as far as we know, we have never seen such a spectral shape for poly(dA) and its derivatives. This is characteristic of the poly(dA)/s-SPG complex. On considering the origin of the CD spectrum in this range, the appearance of the new spectra suggests that the spatial relationship between the adjacent adenine moieties is drastically altered upon the complexation. The movement of the adenine in poly(dA) is achievable because the puckering in poly(dA) is *C2'-endo*. Thus the rotation around the glycosidic bond is allowed. Although determination of the exact torsional angel is impossible from CD data, the vanishing 250 nm negative band (characteristic of *anti* for both *C2'-endo* and *C3'-endo*) suggests that the *syn* form is one possibility for this novel CD pattern in the complex. We can thus conclude that the complexation induces the movement of the adenine from *anti* to a completely new form (maybe *syn*); as a consequence, the CD spectrum is drastically changed on the complexation. The spectral changes upon the complexation for poly(dA) are quite contrast with poly(A) (d-1) in which the complexation does not change the spectral shape but it only enlarges the intensity. This contrast between poly(A) and poly(dA) can be ascribed to the difference in the ribose puckering between poly(A) and poly(dA); therefore, the puckering in poly(A) is *C3'-endo* so that only *anti* is allowed.

At 95 °C in the non-salt and neutral solution, the poly(dA) in the complex undergoes conformational transition HL to H before the dissociation of the complex. Panel (a-2) presents the CD spectrum for H at 60 °C (dotted line), clearly showing considerable difference from HL (dotted line in a-1). Comparing with the CD spectrum of S_{dA}–N_{dA} reported by Olsthoorn *et al.*,[13] H is identical to their spectrum, having a strong negative band at 250 nm and a strong positive band at 260 nm. Therefore, H can be ascribed to a poly(dA) conformation containing *C3'-endo* and *anti* as a minority among the majority of *C2'-endo* and *anti*.

Salt Concentration Dependence of the Poly(dA) Conformation

When we increased KCl concentration at 5 °C (compare (a-1), (b-1), and (c-1) in Figure 3), the poly(dA) spectrum (solid line) increases the intensity around 275 nm with maintaining the 250 nm negative band. This indicates that there is a new conformation in the higher salt solution. Hereinafter, we label it as SA. In comparison of the solid lines between (c-1) and (d-1), the overall spectral shape of SA is quite similar to that of poly(A). In the previous work,[1] poly(A) takes *C3'-endo* and *anti*, so that the similarity suggests that poly(dA) also takes *C3'-endo* and *anti* in the 2 M and 1 M KCl solution. This is a reasonable conclusion from the standpoint that the salts reduce the electrostatic repulsion between the phosphate anions. The distance between the adjacent phosphate anions is about 5.9 Å in *C3'-endo*, while it is 7.0 Å in *C2'-endo*. Therefore, in the non-salt solution, *C2'-endo* is more preferable than *C3'-endo* and this seems the main reason why poly(dA) takes *C2'-endo* in the non-salt solution. When a suitable amount of salts is added, the electrostatic repulsion becomes less important and other factors determine the conformation.

When we examine the salt-concentration dependence of the spectrum for poly(dA) at 5 °C [solid lines in (a-1), (b-1), and (c-1) in Figure 3], the spectrum changes from S_{dA} to SA between 0 and 1 M KCl. The complex maintains HL at 1 M KCl and the spectral change occurs between 1 and 2 M. In 2 M KCl, the spectrum of the complex seems to consist of H and SA. This indicates that the poly(dA) chain in the complex takes almost *C3'-endo* and *anti* in 2 M KCl. When we increased temperature in 2 M KCl, H was maintained and the 275 nm positive band disappeared, indicating that at 2 M KCl, the H conformation dominates at all temperatures. Therefore, there is no conformational transition on heating in the 2 M KCl solution.

Figure 4 summarizes the salt concentration dependence of the CD spectrum of poly(dA)/s-SPG, compared with that of poly(dA). At the low temperature and low salt concentration, the poly(dA) in the complex takes the HL form, which is estimated to be *C2'-endo* with the different torsional angle from the *anti* form. With increasing temperature, HL changes to H, which bears characteristics of *C3'-endo* and *anti* as a minority among the majority of *C2'-endo* and *anti* (*i.e.*, S_{dA}–N_{dA}). When the salt concentration is increased, the spectrum changes to combination of SA and H, with disappearing HL at 5 °C and H form is dominated at 60 °C.

Melting Behavior of the Complex and Comparison with Poly(dA)/Poly(dT) Duplex

Figure 5 compares the temperature dependence of UV absorbance at 257 nm for poly(dA), poly(dA) + s-SPG in non-salt and neutral, and poly(dA) + s-SPG in 2 M NaCl. For poly(dA), the absorbance increases with increasing temperature, due to the decrease in the helix content in the original *C2'-endo* and *anti* form.[1,12,13,16] For poly(dA) + s-SPG in non-salt and neutral, the absorbance at 0 °C is lower than that of poly(dA) because

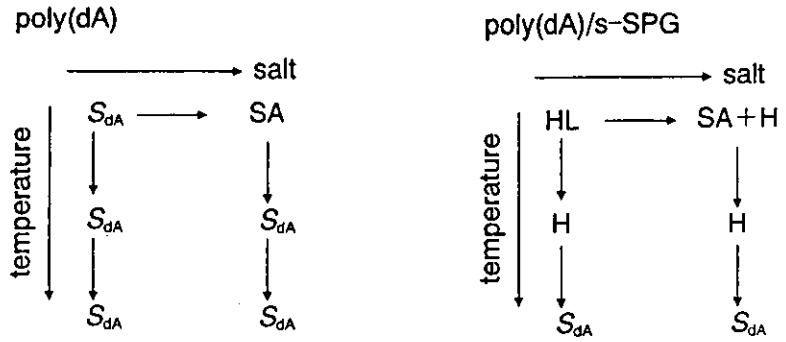

S_{dA}: *C2'-endo and anti* for poly(dA) chain
N_{dA}: *C3'-endo and anti* for poly(dA) chain
HL: high molecular weight and low temperature form, *C2'-endo* in that the torsion of the glycosidic bond is different from S_{dA}, it can be *syn*
H: high temperature form, *C3'-endo and anti* as a minority among the majority of *C2'-endo and anti*
SA: conformation of poly(dA) itself in higher salt concentrations

Figure 4. Summary of the salt concentration dependence of the CD spectrum of poly(dA)/s-SPG, compared with that of poly(dA).

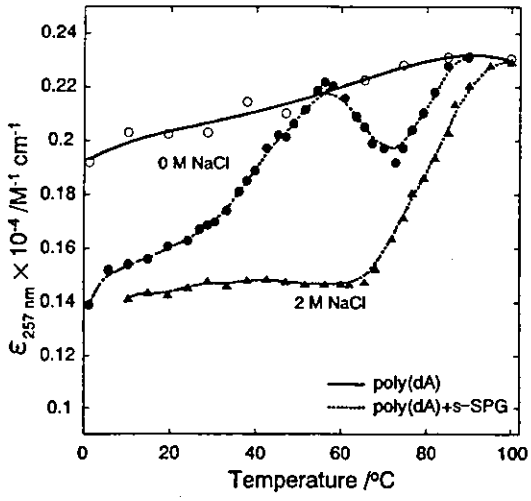

Figure 5. Temperature dependence of UV absorbance at 257 nm for poly(dA), poly(dA) + s-SPG in the non-salt and neutral solution, and poly(dA) + s-SPG in 2 M NaCl.

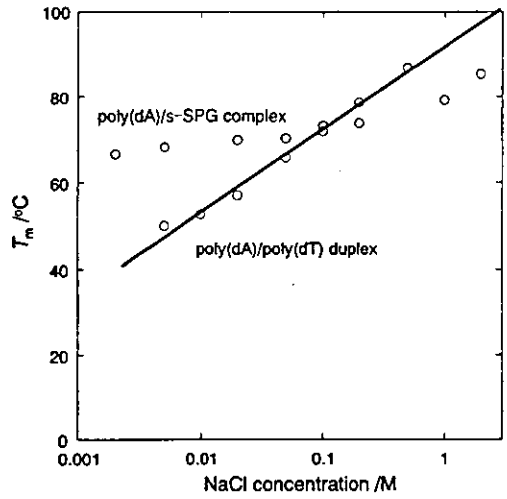

Figure 6. Comparison of NaCl concentration dependence of T_m for poly(dA)/poly(dT) duplex and poly(dA)/s-SPG complex.

of the hypochromic effect due to the complexation. On heating, it stays at a lower value than that of poly(dA) at T = 0–50 °C, then increases to the same value with poly(dA), and again shows the lower absorbance than that of poly(dA) in T = 60–95 °C before the dissociation of the complex. The disappearance of the hypochromic effect is consistent with the conformational transition before melting. In sharp contrast to the non-salt and neutral solution, the complex in 2 M NaCl dose not show such disappearance. There is thus no conformational transition.

Figure 6 plots T_m against NaCl concentration comparing between poly(dA)/s-SPG and poly(dA)/poly(dT). When NaCl concentration is less than 5 mM, there is no hybridization for the poly(dA) + poly(dT) mixtures, Because both poly(dA) and poly(dT) are polyanions, so that the electrostatic repulsion between the cations has to be shielded by salts in order to form the duplex.[1,17,18] With increasing NaCl concentration ([NaCl]), T_m increases 100 °C at [NaCl] = 2 M. T_m of the complex is insensitive to [NaCl], compared to the poly(dA)/poly(dT) duplex. For the complex, T_m increases from 65 to 75 °C when [NaCl] increases from 0 to 2 M. This may be the schizophyllan chain having no electrical-charge so that there is no electrostatic repulsion between s-SPG and poly(dA). The small increment in T_m in the complex is contrast to that of PNA/DNA complex, in that T_m decreases slightly with increasing [NaCl].[19,20] PNA is a peptide nucleic acid in which the phosphodiester backbone has been replaced by a pseudo-peptide chain, so that there is no electronic

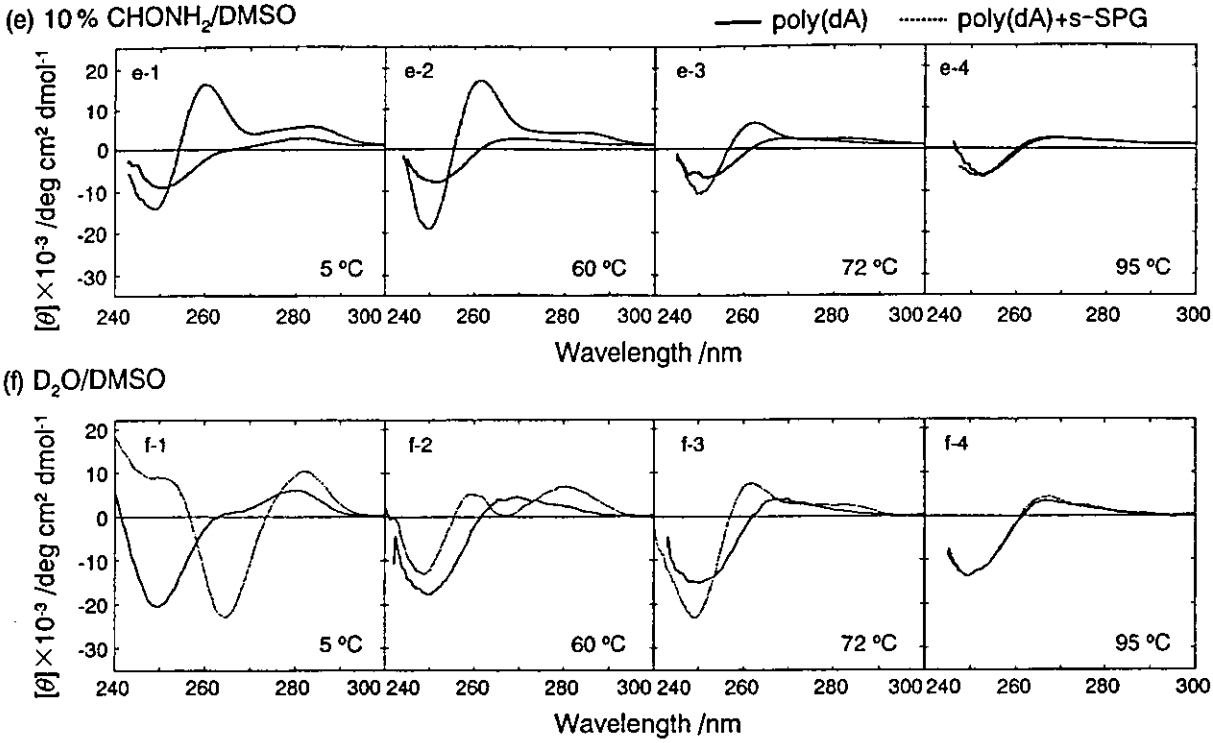

Figure 7. Temperature dependence of the CD spectra for poly(dA) and poly(dA) + s-SPG in (e) 10% formamide and (f) D_2O solution.

change in the chain.[21] The reason for increase T_m with increasing [NaCl] is not clear, but possibly related to the conformational change in poly(dA).

Addition of D_2O or Formamide

Figure 7 shows the temperature dependence of the CD spectra for poly(dA) and poly(dA) + s-SPG in aqueous solution containing 10 vol% formamide/DMSO and in D_2O/DMSO. Formamide cleaves the hydrogen bonding. Poly(dA) decreases the CD intensity at 250 nm, suggesting decrease in the helix content. As shown in (e-1), the CD spectrum of the complex in the formamide solution at 5 °C is quite similar to that of the non-salt and neutral solution at 60 °C. On comparing (e-1) and (a-2), formamide induces the same effect as increasing temperature. The addition of formamide enlarges the H conformation range.

When we exchanged the solvent for D_2O (Figure 7 (f-1)), the CD spectrum at 5 °C is essentially the same as that of the H_2O system. However, the HL form is not replaced by the H form at 60 °C (see (f-2)) and the transition temperature form HL to H can be evaluated to be 72 °C, which is 12 °C higher than that of the H_2O system. Therefore, D_2O induces the same effect as decreasing temperature.

SUMMARY

The relationship between the conformation and solvent for the poly(dA)/s-SPG complex was examined. The diverse and complicated CD spectra for the poly(dA)/s-SPG complex can be explained by the conformational diversity of the ribose puckering and the freedom of the torsional angle of the glycosidic bond for the adenine. This new sight should broaden our horizon to understand the novel interaction between polysaccharides and polynucleotides.

APPENDIX

Figure 8 shows the CD spectral change on heating for the poly(dA)/s-SPG complex. The spectra at 0 °C are different from those reported in the previous paper. The previous HL spectrum had a small negative band at 250 nm, whereas, the present one, a positive shoulder around 250 nm. The low temperature spectrum for poly(dA)/s-SPG (*i.e.*, HL) was subsequently found to depend on annealing conditions. The longer annealing time provides the smaller negative band at 250 nm and one week is sufficient for saturation. In this work, all samples were left at 5 °C for at least one week and longer than one week did not provide an appreciable change in the CD spectrum. As shown in the figure, the spectra obtained in the temperature range of 0–60 °C (upper panel) have isosbestic points at 257 and 280 nm, and those at 65–90 °C (lower panel) have isosbestic points at 254 and 270 nm. The upper panel is totally different from the lower panel. These isosbestic

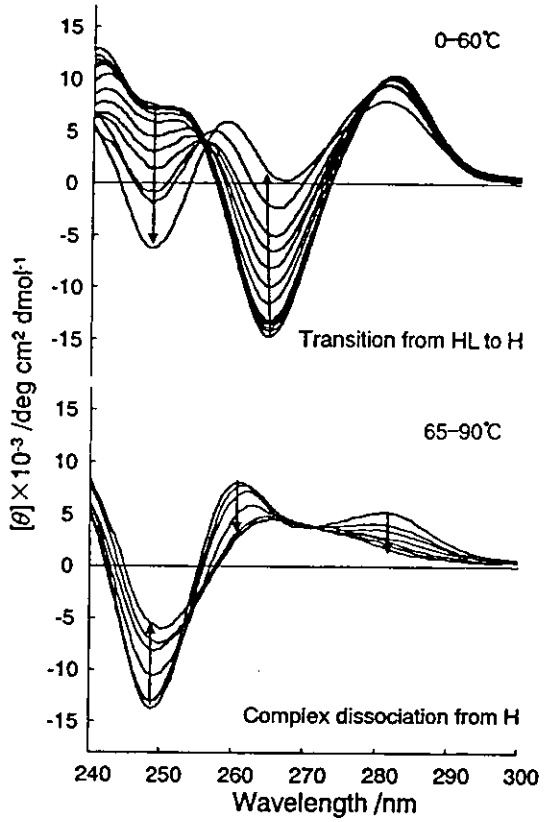

Figure 8. Temperature dependence of the CD spectra for poly(dA)+s-SPG in non-salt and neutral solution. Upper panel shows the changes between 0–60 °C and the lower panel, 65–90 °C.

points indicate that the CD spectrum involves two competing conformations in equilibrium and one conformation becomes dominant on heating. Figure 8 thus confirms the poly(dA) chain in the complex undergoes a conformational transition on heating below T_m of the complex, and the low and high temperature forms are designated as HL and H, respectively.

Acknowledgment. This work is finically supported by the "Organization and Function", PRESTO, and SORST programs in Japan Science and Technology Corporation (JST).

REFERENCES AND NOTES

1. W. Saenger, in "Principles of Nucleic Acid Structure", Springer-Verlag, New York, N.Y., 1984.
2. J. W. Chase and K. R. Williams, *Ann. Rev. Biochem.*, **55**, 103 (1986).
3. M. D. Powell and D. M. Gray, *Biochemistry*, **34**, 5635 (1995).
4. K. Sakurai and S. Shinkai, *J. Am. Chem. Soc.*, **122**, 4520 (2000).
5. K. Tabata, W. Ito, T. Kojima, S. Kawabata, and A. Misaki, *Carbohydr. Res.*, **89**, 121 (1981).
6. T. Norisuye, K. Yanaki, and H. Fujita, *J. Polym. Sci.*, **18**, 547 (1980).
7. K. Yanaki, T. Norisuye, and H. Fujita, *Macromolecules*, **13**, 1462 (1980).
8. T. M. McIntire and D. A. Brant, *J. Am. Chem. Soc.*, **120**, 6909 (1998).
9. M. Mizu, T. Kimura, K. Koumoto, K. Sakurai, and S. Shinkai, *Chem. Commun.*, 429 (2001).
10. K. Sakurai, M. Mizu, and S. Shinkai, *Biomacromolecules*, **2**, 641 (2001).
11. N. Berova, K. Nakanishi, and R. W. Woody, Eds., "Circular Dichroism: Principles and Application", 2nd ed, Wiley-VCH, Canada, 2000.
12. N. Stephen, in "Nucleic Acid Structure and Recognition", Oxford University Press Inc., London, 2002.
13. C. S. M. Olsthoorn, L. J. Bostelaar, J. F. M. Rooij, J. H. van Boom, and C. Altona, *Eur. J. Biochem.*, **115**, 309 (1981).
14. C. S. M. Olsthoorn, L. J. Bostelaar, J. H. van Boom, and C. Altona, *Eur. J. Biochem.*, **112**, 95 (1980).
15. S_{dA} and N_{dA} specifically stand for the *C2'-endo* and *anti* and *C3'-endo* and *anti* conformations for poly(dA) chain.
16. V. V. Filimonov and P. L. Privalov, *J. Mol. Biol.*, **122**, 645 (1978).
17. B. Pullman and A. Pullman, *Progr. Nucl. Acid Res. Mol. Biol.*, **9**, 327 (1969).
18. D. Porschke, *Mol. Biol. Biochem. Biophys.*, **24**, 191 (1977).
19. M. Egholm, O. Buchardt, L. Christensen, C. Behrens, S. M. Freier, D. A. Driver, R. H. Berg, S. K. Kim, B. Norden, and P. E. Nielsen, *Nature*, **365**, 566 (1993).
20. S. Tomac, M. Sarkar, T. Ratilainen, P. Wittung, P. E. Nielsen, B. Norden, and A. Graslund, *J. Am. Chem. Soc.*, **118**, 5544 (1996).
21. P. E. Nielsen and G. Haaima, *Chem. Soc. Rev.*, **26**, 73 (1997).

Available online at www.sciencedirect.com
SCIENCE DIRECT®
Biomaterials 25 (2004) 3117–3123
Biomaterials
www.elsevier.com/locate/biomaterials

Antisense oligonucleotides bound in the polysaccharide complex and the enhanced antisense effect due to the low hydrolysis ☆

Masami Mizu[a], Kazuya Koumoto[a], Takahisa Anada[a], Kazuo Sakurai[a,*], Seiji Shinkai[b]

[a] *Department of Chemical Process & Environments, The University of Kitakyushu, 1-1, Hibikino, Wakamatu-ku, Kitakyushu, Fukuoka 808-0135, Japan*
[b] *Faculty of Engineering Department of Chemistry & Biochemistry, Graduate School of Engineering, Kyushu University, 6-10-1 Hakozaki, Higashi-ku, Fukuoka, Fukuoka 812-8581, Japan*

Received 2 July 2003; accepted 10 November 2003

Abstract

Schizophyllan is a β-(1→3)-D-glucan and can form a novel complex with some single-chains of DNAs. As the preceding paper revealed, the polynucleotide bound in the complex is more stable to nuclease-mediated hydrolysis than the polynucleotide itself (i.e., naked polynucleotide). This paper examined possibility to apply this complex to an antisense DNA carrier, using an in vitro (cell-free) transcription/translation assay. In this assay, we used a plasmid DNA coding a green fluorescence protein (GFP) and an antisense DNA designed to hybridize the ribosome-binding site in the GFP-coded mRNA. When the antisense DNA was administered as the complex, a lower GFP expression efficiency (or higher antisense effect) is observed over naked DNA. This is because the antisense DNA in the complex is protected from the attack of deoxyribonuclease. When exonuclease I, which specifically hydrolyzes single DNA chains, was present in the GEP assay system, the antisense effect was not changed for the complex while being weakened in the naked antisense DNA system. These results imply that the exonuclease I cannot hydrolyze the antisense DNA in the complex, while it can hydrolyze naked DNA to reduce its antisense effect.

Keywords: Antisense; DNA; Gene expression; Polysaccharide; Complexation

1. Introduction

Schizophyllan is an extracellular polysaccharide produced by the fungus *Schizophyllan commune* and the main chain consists of β-(1→3)-D-glucan and one β-(1→6)-D-glycosyl side chain links to the main chain at every three glucose residues [1]. Schizophyllan adopts a triple helix conformation in water and a random coil in dimethylsulfoxide (DMSO) [2,3]. When water is added to the DMSO solution (renaturation), the triple helical structure can be partially retrieved through this process, although the entire chain structure may not be the same with the original triple helix [4,5]. Recently, Sakurai and Shinkai [6,7] found that the schizophyllan single chain (s-SPG[1]) forms a macromolecular complex with some homo-polynucleotides, when the polynucleotide is present in the renaturation process. Their subsequent paper [8] reveals that the polynucleotide bound in the complex is more stable to nuclease-mediated hydrolysis than the polynucleotide itself (i.e., naked polynucleotide), using both high-performance liquid chromatography and ultraviolet absorbance methods. This low hydrolysis of the complex suggests that s-SPG is applicable to an antisense oligonucleotide (AS ODN) carrier.

In this paper, we attempted to further evaluate the capability of the complex to act as an AS ODN carrier, using the pQBI63 vector as a reporter gene in *Escherichia coli* T7 S30 extract solutions. The pQBI63 vector contains the gene to code a red-shifted green fluorescence protein [9–11] (hereinafter we simply call it GFP) and the GFP-coding region is under the control of a T7 promoter [11]. Since the *E. coli* T7 S30 extract solution contains the T7 RNA polymerase, essential amino acids, and other all necessary components for translation, once the pQBI63 was added to the extract solution, the GFP-coding mRNA is produced, and subsequently GFP is produced. This system is called "in vitro cell-free transcription/translation assay" and

☆This paper is the 20th paper in the series of polysaccharide/polynucleotide complexes.

*Corresponding author.
E-mail address: sakurai@env.kitakyu-u.ac.jp (K. Sakurai).

[1] In this paper, s-SPG and t-SPG stand for single chain of schizophyllan and natural triple helix of schizophyllan, respectively.

0142-9612/$ - see front matter © 2003 Elsevier Ltd. All rights reserved.
doi:10.1016/j.biomaterials.2003.11.008

have been shown very useful for antisense assays [12–14]. We applied this established assay method to our s-SPG complex to evaluate how the complex enhances the antisense effect.

2. Experimental

2.1. Materials

Taito Co. Ltd. (Japan) kindly supplied a fractionated triple-helix schizophyllan sample. The weight-average molecular weight (M_w) and the number of repeating units were found to be 1.5×10^5 and 231, respectively [6,7]. Polyethyleneimine (PEI) with 80 kDa (Fluka), dextran ($M_w = 10^5$) (Wako), and amylose ($M_w =$ 2800) (Wako) were used without further purification. *E. coli* SK4258 originated exonuclease I (Exonuclease I) was purchased from Pharmacia. The pQBI63 vector was purchased from Takara, and the *E. coli* T7 S30 extract solutions were purchased from Promega [12] and Novagen [15]. The antisense sequence (CTTTAAGAAGGAGATATACAT) was used to hybridize the ribosome binding site (the antisense of binding site is underlined, see Table 1) [13,16]. We found that s-SPG cannot bind the antisense sequence itself, because of the short sequence length [17]. Since we already knew that a certain length of poly(dA) is necessary to bind to s-SPG [17], we added a poly(dA) tail [poly(dA)$_{20}$ or poly(dA)$_{40}$] to the end of the antisense sequence as shown in Table 1 and used four different AS ODN samples (denoted by ANT1, ANT2, ANT3 and ANT4). All AS ODN samples were synthesized at Hokkaido System Science (Japan).

2.2. DNA complexation

50 μg of each ANT sample (i.e., ANT1, ANT2, ANT3 and ANT4) was dissolved in 10 mM Tris buffer (pH 8.0) containing 50 mM KCl. A s-SPG/DMSO solution with an appropriate concentration was added to each ANT solution so that the water volume fraction was always 0.9 after mixing. In most cases, the molar ratio ($M_{s\text{-SPG}}/M_{ANT}$) was controlled to 1.0, where $M_{s\text{-SPG}}$ and M_{ANT} are the repeating molar concentrations of s-SPG and ANT, respectively. Only for ANT1, $M_{s\text{-SPG}}/M_{ANT}$ was changed to 0.1, 0.25, 0.5, 0.75, 1.0, 2.0, 3.0, and 4.0 in order to optimize experimental conditions. After the s-SPG + ANT[2] mixture was left at 5°C for 24 h to allow the complex to form, DMSO was removed by ultra-filtration (3000 M_w cut off, Millpore). After filtration, the final concentration of ANT was determined by ultraviolet absorbance.

[2] In this paper, s-SPG + ANT stands for a mixture of ANT and s-SPG, and does not necessary mean the complex. This can be just a mixture of the two components without any complexation. In fact, s-SPG + ANT2 does not form a complex. However, the ANT1, ANT3 and ANT4 mixtures essentially only consist of s-SPG/ANT complexes [8].

Table 1
AS ODN samples and their sequences used in this study

Name	Sequence	Size (bases)
Antisense	CTTTAAGAAGGAGATATACAT	21
ANT1	CTTTAAGAAGGAGATATACAT-dA$_{40}$	61
ANT2	dA$_{20}$-CTTTAAGAAGGAGATATACAT-dA$_{20}$	61
ANT3	dA$_{40}$-CTTTAAGAAGGAGATATACAT-dA$_{40}$	101
ANT4	dA$_{40}$-CTTTAAGAAGGAGATATACAT	61

The binding site is underlined, which is designed to hybridize the ribosome binding site of the T7 promoter system [13,14,16].

The preceding paper [8] employed gel electrophoresis and spectroscopic methods to show that s-SPG can form complexes with both ANT1 and ANT2, while ANT3 cannot. This difference in the complexation ability is ascribed to differences in the length of the poly(dA) tail [17]. We did not directly examine whether ANT4 forms the complex since ANT4 has the considered poly(dA)$_{40}$ tail on its 5′ end.

2.3. In vitro transcription/translation assay

A known in vitro cell-free transcription/translation assay was performed, using the pQBI63 vector in *E. coli* T7 S30 extract solutions (Promega or Novagen). The pQBI63 was amplified in *E. coli BL21(DE3)* (Novagen) and purified with a Plasmid Midi Kit (Qiagen). 1 μg of pQBI63 plasmid was added to 50 μl of the *E. coli* T7 S30 extract solution and the resultant solution was incubated at 37°C. In this condition, after 30 min, the plasmid DNA (i.e., pQBI63) started to express a sufficient amount of GFP, enough to provide appreciable fluorescence intensity. We adopted this protocol as the standard. To evaluate ANT/carrier antisense effects, the ANT samples or their s-SPG complexes were added to the standard. Usually, 10 μg of ANT was added to the standard. The total amount of the carrier complex was changed so as to maintain 10 μg of total ANT in an assay. The amount of GFP expressed was evaluated as the fluorescence intensity at 507 nm (excited at 463 nm) with a Hitachi F4500 fluorescence spectrometer.

According to Promega Technical Notes [18], "linearization significantly reduces the expression of the luciferase gene in the T7 S30 system. This reduction is a result of exonuclease activity in the T7 S30 system". Therefore, Promega's *E. coli* T7 S30 extract solution contains some amount of nuclease. This situation is convenient to examine how the s-SPG/ANT complex protects the bound AN ODNs from nuclease-mediated hydrolysis. Thus, we decided to compare antisense

effects between naked ANT and the s-SPG/ANT complex using the Promega *E. coli* T7 S30 system.

In the next step, we examined the antisense effect when intentionally added Exonuclease I (0.2 or 0.5 units/ml) to the system. This examination needed a completely nuclease-free (or nuclease-inhibited) T7 S30 extracted solution. For this purpose, we used Novagen's *E. coli* T7 S30 extract solution. According to their technical note [15] (EcoPro™ System), "The EcoPro System will function with a variety of DNA templates containing T7 or *E. coli* promoters upstream from coding sequence, including super-coiled, liner DNA and PCR products." Therefore, Novagen's *E. coli* T7 S30 extract solution can be considered practically nuclease-free. In fact, our data (Fig. 4) confirm that there is no detectable amount of active nuclease left in the extract solution.

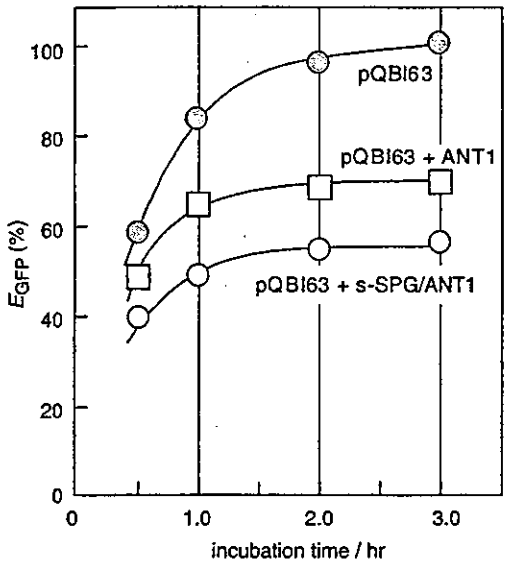

Fig. 1. Anti-sense affects on GFP expression efficiency (E_{GFP}) during incubation at 37°C in the *E. coli* T7 S30 extract system (Promega). pQBI template DNA system (control), filled circles; pQBI + ANT1, unfilled squares; pGBI + ANT1/s-SPG, unfilled circles. 1 μg of pQBI 63 was added to 50 μl of *E. coli* extract solution and incubated. E_{GFP} is defined by dividing the measured fluorescence intensity by that of the control (incubated for 3 h).

3. Results and discussion

3.1. Antisense effect and incubation time

To determine the optimal incubation time to compare antisense effects, the following three typical systems: pQBI63 itself (control), a mixture of pQBI63 and ANT1 (naked AN ODN), and a mixture of pQBI63 and s-SPG/ANT1 (complex) were examined. We added each of them to Promega's *E. coli* T7 S30 extract solution and measured GFP expression efficiency (E_{GFP}) against incubation time. The results are presented in Fig. 1. Here, E_{GFP} is defined by dividing the measured fluorescence intensity of each assay by that of the control incubated for 3 h. As shown in the figure, GFP expression seems saturated after 2–3 h. When three combinations are compared after 3 h, E_{GFP} for the naked ANT1 (in the figure denoted by pQBI63 + ANT1) is reduced to 70% of the control, and to 50% of the control for the pQBI63 + s-SPG/ANT1 complex. Although the data are not plotted, a mixture of pQBI63 and s-SPG (without ANT) shows almost the same features as the control, indicating that the presence of s-SPG in the system provides no influence on GFP expression (see below for details).

In the *E. coli* T7 S30 extract solution, sufficient amounts of NTP (nucleoside triphosphates), essential amino acids as well as other necessary components for protein expression exist [12]. Furthermore, AN ODNs should not consume those components or inhibit their functions, except through the GFP expression. Therefore, the saturated values of E_{GFP} in Fig. 1 should reflect the total amount of the mRNA translated to GFP. Thus, lower E_{GFP} values for pQBI63 + s-SPG/ANT1 and pQBI63 + ANT1 over controls can be explained by antisense effects [13,14]. Furthermore, differences between pQBI63 + ANT1 and pQBI63 + s-SPG/ANT1 should be related to the presence of the complex. After incubation for 3 h, E_{GFP} seems saturated for all three systems. Therefore, hereinafter, only E_{GFP} after incubation for 3 h was compared.

3.2. Comparison of the GFP expression efficiency using carriers and ANTs

Fig. 2 summarizes GFP expression efficiencies (E_{GFP}) (incubation time is 3 h for all measurements; E_{GFP} is defined by dividing the measured fluorescence intensity by that of the control). The control is indicated as the filled bar [pQBI63, Control (1)] in the histogram of Fig. 2. To examine whether polysaccharides interfere with the assay system, we added 50 μg of each polysaccharide (dextran, amylose, triple helix of schizophyllan or single chain of schizophyllan) to the standard: Fig. 2 assays (2)–(5). By comparing them, it is clear that simple presence of those polysaccharides does not provide any interference to normal GFP expression. When we added each ANT sample to the standard (ANT1;(6), ANT2;(7) and ANT3 (8)), values for E_{GFP} are reduced to about 75% of the control. This reduction should be ascribed to antisense effects. There is no significant difference among the three ANT samples, showing that the antisense effect is nearly the same for all three samples. The assays from (9) to (16) present the $M_{s\text{-}SPG}/M_{ANT}$ dependence of E_{GFP} for the ANT1 + s-SPG system. This series of assays shows that

E_{GFP} decreases with increasing the s-SPG molar ratio, and reaches a minimum at $M_{s\text{-}SPG}/M_{ANT} = 1.0$, then increases. When $M_{s\text{-}SPG}/M_{ANT} \geq 4$, the assay solution was opaque due to precipitation. Poor solubility or precipitation was sometimes observed when the assay mixture contained excess s-SPG to polynucleotides. The increment in E_{GFP} in the assays (14)–(16) in Fig. 2 can be ascribed to presence of the insoluble component of the complex. Since the lowest E_{GFP} is attained at $M_{s\text{-}SPG}/M_{ANT} = 1$, all measurements were carried out at this composition (including the preliminary examination in Fig. 1).

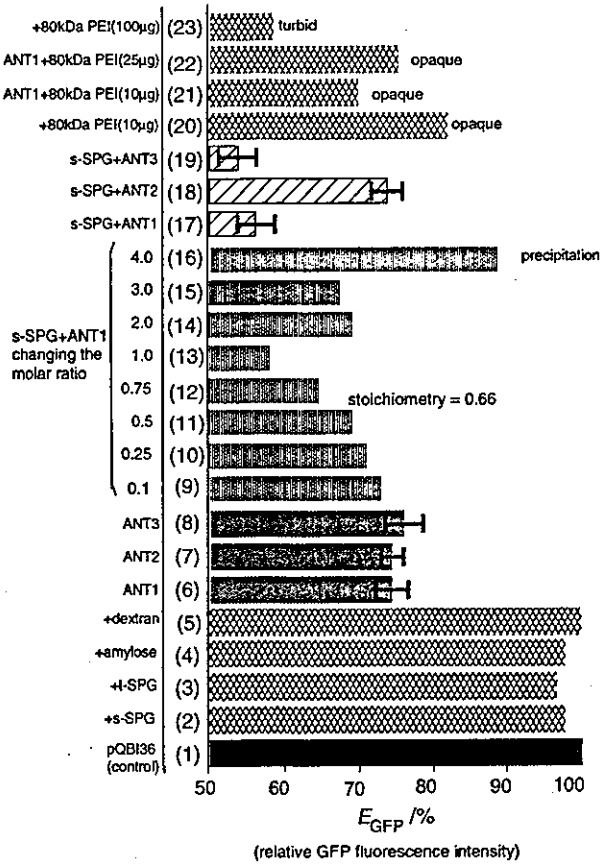

Fig. 2. Comparison of GFP expression efficiency (E_{GFP}) after incubation for 3 h, assay (1): pQBI template DNA only (control), 1 μg of pQBI 63 added to 50 μl of *E. coli* extract solution. Assays (2)–(5): each polysaccharide (100 μg) was added to the reference, t-SPG and s-SPG refer to triple helix and single chains of schizophyllan, respectively. Assays (6)–(8): 10 μg of each ANT was added to the standard. Assays (9)–(16): the mixture of s-SPG and ANT1 (complexes formed) were added to the standard numbers on the left-hand side show the $M_{s\text{-}SPG}/M_{ANT}$ molar ratio. Assays (17)–(19): comparison of ANT1 + s-SPG (complex), ANT2 + s-SPG (no complex), and ANT3 + s-SPG (complex). (20): 10 μg of 80 kDa PEI (polyethyleneimine) was added to the standard. Assay (21): 10 μg of ANT1 was mixed with 10 μg of 80 kDa PEI and the mixture was added to the standard. Assay (22): 10 μg of ANT1 was mixed with 25 μg of 80 kDa PEI and the mixture was added to the standard. Assay (23): 100 μg of 80 kDa PEI was added to the standard.

As already shown [8], ANT2 cannot bind the s-SPG due to the short poly(dA) tail. This fact can then explain why there is no difference in E_{GFP} between naked ANT2 (assay (7)) and the mixture of ANT2 and s-SPG (assay (18)). On the other hand, ANT1 and ANT3 do form complexes with s-SPG. When ANT1 and ANT3 are added as the complex (assays (17) and (19)), E_{GFP} is drastically reduced. To confirm whether these differences in E_{GFP} between naked ANTs and complexed ANTs are statistically different from each other, we calculated the dispersion and *t*-value (Table 2). The results clarifies that the averaged E_{GFP} between naked ANTs and complexed ANTs are statistically different. The Promega *E. coli* T7 S30 extract solution is well-known to contain some amount of nuclease. Thus, protein expression from liner DNAs is significantly reduced because of DNA hydrolysis [18]. Therefore, when ANTs are added to this system, they should also suffer hydrolysis from intrinsic nuclease activity. Our previous paper revealed that nuclease-mediated hydrolysis of polynucleotides is drastically reduced in the complex [8]. Furthermore, we have directly proven that both s-SPG/ANT1 and s-SPG/ANT3 complexes show a lower hydrolysis rate than the corresponding naked ANTs [8]. Considering these two facts (presence of nuclease in the system, and low hydrolysis of complexed nucleotides), the low E_{GFP} for the complex can be explained by s-SPG protection of bound ANT and increased amount of ANT to bind mRNA, resulting to prohibit GFP expression.

PEI is used as an AS ODN positive control carrier, with 10 μg of PEI to 1 μg of pQBI63, and determination of E_{GFP}. As shown in Fig. 2, assay (20), E_{GFP} is reduced to 80%. It should be pointed out that even though no ANT is present, E_{GFP} is decreased in this PEI case. We also found that the solution becomes slightly opaque when PEI is added to the pQBI63 solution. This is probably due to complexation between cationic PEI and anionic pQBI63. Therefore, the observed reduced E_{GFP}

Table 2
Statistical analysis of the antisense test for the assays (6)–(7) and (17)–(19) in Fig. 2

	ANT1	ANT1 + s-SPG	ANT2	ANT2 + s-SPG	ANT3	ANT3 + s-SPG
Average	56.4	74.5	74.0	75.3	54.0	75.3
Dispersion	4.3	4.3	2.5	2.9	6.5	4.3
n	5	4	5	4	5	4
t-value	15.1		3.9		15.4	

can be ascribed to the reduced plasmid. This interaction becomes more prominent when 100 μg of PEI are added to 1 μg of pQBI63, thus E_{GFP} in assay (23) is lower than that of assay (20). Polyion complexes between ANT1 and PEI according to a literature protocol [19] produce antisense effects, in assays (21) and (22). When 10 μg of ANT1 and 10 μg of PEI are mixed (assay 21), E_{GFP} was reduced to 70%. This means that the same antisense effect is present in the presence of PEI to some extent. However, when PEI is increased to 25 μg (assay 22), the solution becomes more turbid than assay 21 and E_{GFP} increases. PEI is known as an AN ODN carrier; however, poor solubility is a problem [19,20]. The present work confirms this problem in PEI and shows the superiority of s-SPG as an AN ODN carrier.

3.3. Nuclease protection mechanism

Fig. 3 compares E_{GFP} when Exonuclease I was intentionally added to the Promega *E. coli* T7 S30 extract solution. Results show that E_{GFP} is unchanged for the complex (indicated by "protection by s-SPG" in the figure). On the other hand, it is increased for naked ANT1. Since Exonuclease I specifically hydrolyzes DNA single-chains, ANT1 suffers serious hydrolysis when Exonuclease I is added, accounting for E_{GFP} increase with the addition. It is interesting that there is no difference in E_{GFP} when Exonuclease I is added to the ANT1/s-SPG complex. This feature suggests that ANT1 is protected from nuclease hydrolysis by the complex.

To examine how the s-SPG complex protects bound AS ODNs, we performed on antisense assay in a nuclease-free *E. coli* T7 S30 extract solution. Novagen's *E. coli* T7 S30 extract solution is available for linear DNAs and PCR products, which means it must be practically nuclease-free or inhibited [15]. The assay results are presented in Fig. 4. Here, we used the same

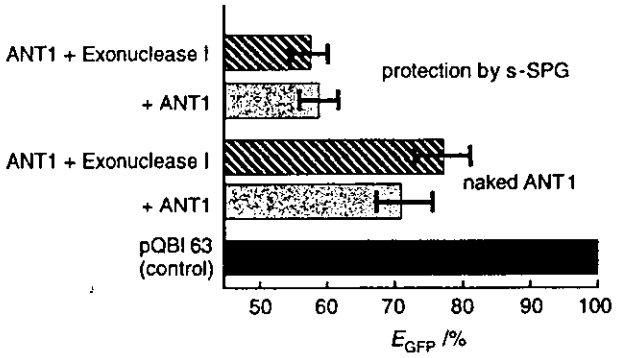

Fig. 3. Comparison of GFP expression efficiency (E_{GFP}) between the ANT1/s-SPG complex and naked ANT1 when Exonuclease I was added to the standard.

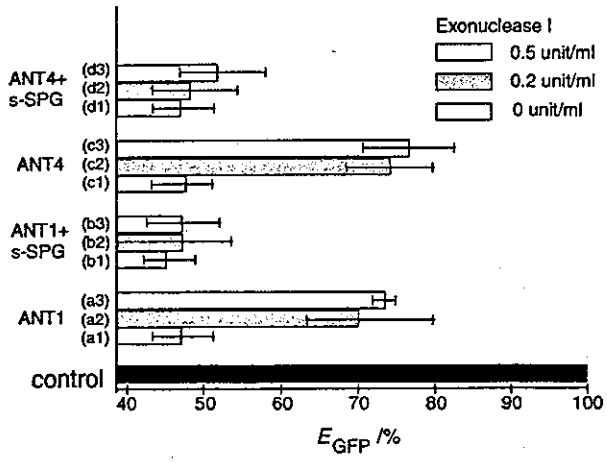

Fig. 4. Effect of addition of Exonuclease I on E_{GFP}, comparing naked ANT and the ANT/s-SPG complexes. Control: pQBI template DNA in Novagen's *E. coli* T7 S30 extract solution. 0.2 and 0.5 unit/ml Exonuclease I was added to the naked ANT1: (assays a2, a3), to naked ANT4: (assays c2, c3), to the s-SPG/ANT1 complex: (assays b2, b3) and to the s-SPG/ANT2 complex: (assays d2, d3).

conditions as those of Figs. 2 and 3, except for using ANT4 and Novagen's *E. coli* T7 S30 extract solution. When Exonuclease I was not present the values for E_{GFP} are almost identical for naked ANTs and their complexes (assays (a1), (b1), (c1) and (d1)). This feature is different from results in Fig. 2, confirming that Novagen's *E. coli* T7 S30 extract solution is practically nuclease activity-free. When Exonuclease I was added to the system, E_{GFP} is increased for the naked ANTs: (assays (a2, a3) and (c2, c3)) as expected. On the other hand, E_{GFP} is unchanged by addition of Exonuclease I for the complex: (assays (b2, b3) and (d2, d3)). These results support that the s-SPG complex protects the bound AS ODNs to a great extent.

ANT1 has the poly(dA) tail at the 3′ end, while ANT4 has this tail at the 5′ end. Exonuclease I hydrolyzes single strand DNA from the 3′ end. Therefore, when exposed to Exonuclease I, ANT4 is expected to be more susceptible to hydrolysis and inactivation than ANT1. In fact, when Fig. 4 assays (a1–a3) are compared with (c1–c3) carefully, E_{GFP} is increased more for the naked ANT4 than naked ANT1. This difference is ascribed to that position difference of the antisense vs. poly(dA) sequence. Additionally, we have evidence to prove that a stable complex is formed between poly(dA) and s-SPG [17], and that the short antisense sequence itself (see Table 1) does not bind specifically to s-SPG. However, for the ANT-poly(dA) fused DNA we do not know whether the hetero sequence component of ANT1 or ANT4 is involved in the complex. If the hetero sequence (i.e., antisense part) is not involved in the complex, it should be more vulnerable than the poly(dA) tail to nuclease digestion In particular, the antisense sequence

located at 3′ end of ANT4 should be the most vulnerable part because Exonuclease I hydrolyzes from this end. However, no significant difference in E_{GFP} is observed between ANT1 + s-SPG and ANT4 + s-SPG(see Fig. 3 assays (b1–b3) and (d1–d3)). One explanation is that the protective s-SPG complexed close to the heterosequence spatially hinders Exonuclease I approach to the DNA. From only this result, it may be premature to conclude that the heterosequence is involved in the complex between the poly(dA) tail and s-SPG.

To sum the AS ODN protection mechanism proposed for the preset system, Fig. 5 schematically presents our model. Once the AS ODN and s-SPG complex is formed, it protects the bound AS ODN from nuclease attack. Survival of the AS ODN to complex target mRNA is increased, thus inhibitis GFP expression over that observed in the naked AS ODN system. This model supposes that the complexed AS ODN is released form the complex when it meets the target mRNA, which means that the binding constant of s-SPG/AS ODN must be less than that of AS ODM/target mRNA. In fact, we found that takeover reaction from s-SPG/poly(A) to poly(A)/poly(T) can be completed in 20 min, suggesting our hypothesis being right. We have clarified this issue in the related paper [21].

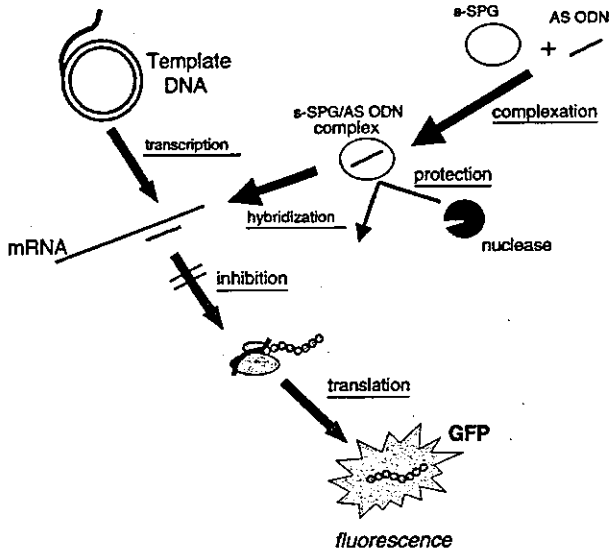

Fig. 5. A schematic illustration to explain the enhanced antisense effect observed in the present system. The template DNA (pQBI63) produces the GFP-coding mRNA by transcription and the mRNA is translated to GFP. When AS ODN (antisense oligonucleotide) is added to this system, the AS ODN binds to the mRNA, inhibiting translation. However, some AS ODNs are hydrolyzed by nuclease. When s-SPG is added to AS ODN, they form a complex. Complexes between AS ODN and s-SPG protect the bound AS ODN from nuclease attack. Levels of intact, surviving AS ODN reaches the target mRNA are increased. This means that inhibition of GFP expression is more enhanced than for the naked AS ODN system.

4. Concluding remarks

We conclude that s-SPG/AS ODN complexes are useful as antisense DNA carriers to reduce nuclease-mediated hydrolysis. We successfully demonstrate that AS ODNs in the s-SPG complex exhibit reduced GFP expression efficiency (or higher antisense effects) than that of naked DNA. When Exonuclease I, which specifically hydrolyzes single DNA chains, was present in the assay system antisense effects are unchanged for the complexes, but significantly weakened in the naked antisense DNA system.

Acknowledgements

This work is financially supported by "Organization and Function", PRESTO, and SORST programs in Japan Science and Technology Corporation (JST).

References

[1] Tabata K, Ito W, Kojima T. Ultrasonic degradation of schizophyllan, an antitumor polysaccharide produced by Schizophyllum commune fries. Carbohydr Res 1981;89:121–35.
[2] Norisuye T, Yanaki T, Fujita H. Triple helix of a Schiphyllum commune polysaccharide in aqueous solution. J Polym Sci Polym Phys Ed 1980;18:547–58.
[3] Yanaki T, Norisuye T, Fujita H. Triple helix of Schizophyllum commune polysaccharide in dilute solution. 3. hydrodynamic properties in water. Macromolecules 1980;13:1462–6.
[4] Sato T, Sakurai K, Norisuye T, Fujita H. Triple helix of Schizophyllum commune polysaccharide in dilute solution. Part VI. Collapse of randomly coiled schizophyllan in mixtures of water and dimethylsulfoxide. Polymer J 1983;15:87–96.
[5] McIntire TM, Brant DA. Observation of the (1→3)-b-D-glucan liner triple helix to macrocycle interconversion using non-contatct atomic force microscopy. J Am Chem Soc 1998;120:6909–19.
[6] Sakurai K, Shinkai S. Molecular recognition of adenine, cytosine, and uracil in a single-stranded RNA by a natural polysaccharide: schizophyllan. J Am Chem Soc 2000;122(18):4520–1.
[7] Sakurai K, Mizu M, Shinkai S. Polysaccharide-polynucleotide complexes. 2. Complementary polynucleotide mimic behavior of the natural polysaccharide schizophyllan in the macromolecular complex with single-stranded RNA and DNA. Biomacromolecules 2001;2(3):641–50.
[8] Mizu M, Koumoto K, Kimura T, Sakurai K, Shinkai S. Protection of polynucleotides from nuclease-mediated hydrolysis by forming a complex with schizophyllan. The preceding submission.
[9] Chalfie M, Tu Y, Euskirchen G, Ward WW, Prasher DC. Green fluorescent protein as a marker for gene expression. Science 1994;263:802–5.
[10] Technical data in Takara manual of GFP, BFP vectors, 2000 (Japanese).
[11] AFPs™ AutoFlouresence Proteins, AFP-Manual (version AFP11-No98), 2001.
[12] Promega, Part# TB219. *E. coli* T7 S30 extract system for circular DNA, 2002.

[13] Murata M, Kaku W, Anada T, Soh N, Katayama Y, Maeda M. Thermo responsive DNA/polymer conjugate for intelligent antisense strategy. Chem Lett 2003;32:266–7.
[14] Anada T, Kano T, Kaku W, Katayama Y, Maeda M. Functional regulation of biomolecule using DNA conjugate. Nucleic Acid Res Suppl 2002;2:269–70.
[15] Novagen EcoPro™ System TB278 06.
[16] 2000 Novagen Catalog. p. 180, http://www.novagen com.
[17] Mizu M, Kimura T, Koumoto K, Sakurai K, Shinkai S. Thermally induced conformational-transisiton of polydeoxyadenosine in the complex with schizophyllan and the base-length dependence of its stability. Chem Commun 2001;429–30.
[18] Atale for four systems, optimized gene expression with the T7 sample system. Promega Note. Number 80, 2002.
[19] Boussif O, Lezoualc'h F, Zanta MA, Mergny MD, Scherman D, Demeneix B, Behr JP. A versatile vector for gene and oligonucleotide transfer into cells in culture and in vivo: polyethylenimine. Proc Natl Acad Sci USA 1995;92:7297–301.
[20] Chirila TV, Rakoczy PE, Garrett KL, Lou X, Constable IJ. The use of synthetic polymers for delivery of therapeutic antisense oligodeoxynucleotides. Biomaterials 2002;23(2):321–42.
[21] Koumoto K, Mizu M, Sakurai K, Kunitake T, Shinkai S. Intelligent release of the single-stranded DNA bound in the schizophyllan complex. Chem Biodiversity, submitted.

Polysaccharide/Polynucleotide Complexes

Part 6

Complementary-Strand-Induced Release of Single-Stranded DNA Bound in the Schizophyllan Complex

by **Kazuya Koumoto**[a]), **Masami Mizu**[a]), **Kazuo Sakurai***[a]), **Toyoki Kunitake**[a]), and **Seiji Shinkai***[b])

[a]) Department of Chemical Processes and Environments, Faculty of Environmental Engineering, The University of Kitakyushu, 1-1 Hibikino, Wakamatsu-ku, Kitakyushu, Fukuoka 808-0135, Japan. (Phone: +81-93-695-3298; fax: +81-93-695-3390; e-mail: sakurai@env.kitakyu-u.ac.jp)

[b]) Department of Chemistry and Biochemistry, Graduate School of Engineering, Kyushu University, Fukuoka 812-8581, Japan.

Spectroscopic properties of single-stranded DNA/schizophyllan ternary complexes (ss-DNA·2s-SPG), induced by addition of either complementary or noncomplementary strands, have been investigated. The addition of the complementary strands to ss-DNA·2s-SPG induced the quick release of the bound ss-DNA to the complementary strands (both DNA and RNA), whereas the ternary complex was unaffected upon addition of noncomplementary strands. Our experiments imply that SPG has complexation properties indispensable to the gene carriers. As far as we know, there is no report on exploitation of such nonviral gene carriers that can accomplish an intelligent release of the bound ss-DNA toward the complementary strands. We believe, therefore, that SPG, a natural and neutral polysaccharide, has a great potential to become a new ss-DNA carrier.

Introduction. – Schizophyllan (SPG) is an extracellular polysaccharide produced by the fungus *Schizophyllum commune*. The main chain of SPG consists of β-1,3-glucan, and every third glucose unit has a β-1,6-glucosidic side chain [1][2]. The three chains are twisted together to form a triple helix (t-SPG) in H_2O, in which strong H-bonds among the 2-OH groups are formed in the main chain [3–6]. It is known that the t-SPG chain dissociates into a single chain of SPG (s-SPG), when dissolved in a denaturing solvent such as dimethylsulfoxide (DMSO) [7][8], and that the triple-helical structure can be restored by exchanging DMSO for H_2O (*Fig. 1*) [9–11]. Such a unique property has been made use of in the food and pharmaceutical industry, and for other purposes [12–14].

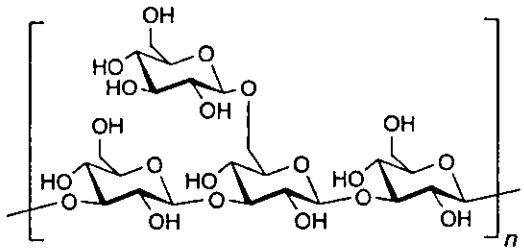

Schizophyllan

Recently, we found that when the renaturation process is carried out in the presence of certain single-stranded (ss) polynucleotides, s-SPG forms macromolecular com-

plexes with the polynuclotides, as schematically shown in *Fig. 1* [15]. Interestingly, the complex dissociates in a cooperative manner upon heating, as if the polysaccharide chain lacking any nucleobase behaves as the complementary strand [15][16]. In addition, taking into consideration that *1*) these complexes possess different melting temperatures [17] and *2*) the minimum base length of polynucleotides to form complexes is different in each nucleobase [17][18], it is clear that the H-bonding interaction between polysaccharides and nucleobases plays an important role in complex formation [16]. To the best of our knowledge, this is the first time that specific interactions between neutral polysaccharides and polynucleotides has been evidenced experimentally. Our further studies have clarified some of the novel properties on the complex: *1*) polysaccharides possessing the β-1,3-glucan main-chain structure can form similar complexes [19][20]; *2*) according to stoichiometric studies, the complex consists of one polynucleotide chain and two polysaccharide chains [16]; and *3*) the polynucleotide chain bound in the complex is resistant against enzymatic hydrolysis [21].

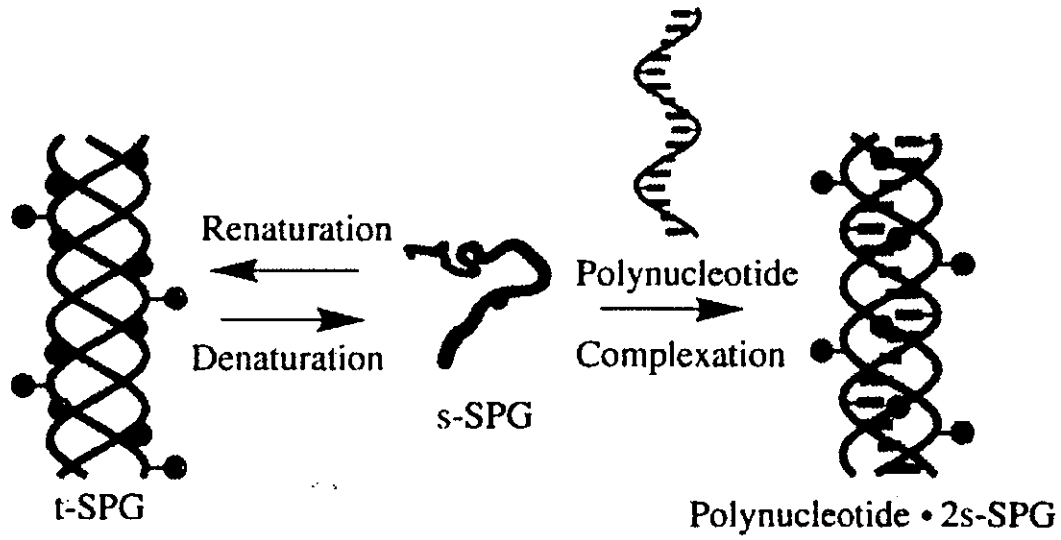

Fig. 1. *Schematic illustration of the equilibria involved in the formation of the triple-helical complex between a polynucleotide and schizophyllan* (s-SPG)

Complex formation and dissociation can be controlled either by changing the pH of the medium [22] or the ion species [23]. These properties are expected to be favorable for industrial or biological applications such as gene separation and gene carriers. To exploit the ability of these complexes as gene carriers, we added the complementary strand to the ss-DNA/s-SPG complex (ss-DNA · 2s-SPG) and observed the spectroscopic changes induced by the addition of the complementary strands. For the peptide nucleic acids (PNA) reported by *Nielsen* and co-workers [24–26], it is known that the incorporation of PNA into double-stranded DNA induces the displacement of the strands, resulting in the formation of DNA · PNA hybrids. In comparison to PNA, the interaction between SPG and DNA (or RNA) is weaker, because the polysaccharide does not provide any *Watson–Crick* or *Hoogsteen* base pairing. It is expected,

therefore, that the addition of the complementary strands to the ss-DNA·2s-SPG complex would induce properties different from those of the PNA and DNA systems.

Results and Discussion. – *Relationship between Circular-Dichroism* (CD) *Spectra and DNA Conformation.* In this study, we chose the poly(dA·2s-SPG) complex as a model system because *1*) the complex has the highest melting temperature among the ss-polynucleotide·2s-SPG complexes ($T_m = 74°$, [NaCl] = 150 mM) [27] and, therefore, is considerably stable under physiological conditions, and *2*) the CD spectra of poly(dA) change drastically upon complexation with s-SPG [18][27]. These properties should make it easy to observe the spectroscopic changes induced by the addition of the complementary strands to ss-DNA·2s-SPG. In general, it is rather difficult to judge duplex formation only from a change in the corresponding CD spectra. Therefore, we first evaluated the relationship between the CD spectral change in the poly(dA)/poly(dT) system and their conformation by both UV and fluorescence spectroscopy. In *Fig. 2, a*, the CD spectral changes upon duplex formation, induced by NaCl, of a mixture of poly(dA) and poly(dT) are shown. At NaCl concentrations lower than 3 mM, the CD spectrum showed only two bands, a positive one at 280 nm, and a negative band at 247 nm. With increasing NaCl concentration, the CD spectra drastically changed: the negative 247-nm band became more intense, and two new maxima appeared at 257 and 263 nm, respectively. We plotted the CD intensity of the characteristic 247-nm band (Θ_{247}) against the NaCl concentration, as shown in *Fig. 2, b*. As can be seen, there is a strong decrease in Θ_{247} at 3–5 mM NaCl concentration, and then a plateau is reached above 5 mM.

In order to assign the above CD spectral changes, we also recorded UV spectra at varying NaCl concentrations. As shown in *Fig. 2, c*, the UV absorbance decreased with increasing NaCl concentration, which can be ascribed to a hypochromic effect due to duplex formation. This absorbance change also supports the view that poly(dA) and poly(dT) form the duplex at NaCl concentrations above *ca.* 5 mM.

Fluorescence spectroscopy is another useful technique to evaluate duplex formation. For example, ethidium bromide can intercalate into a poly(dA·dT) duplex, giving rise to strong fluorescence ($\lambda_{ex} = 330$ nm, $\lambda_{em} = 590$ nm). In *Fig. 2, d*, the relative fluorescence intensity of ethidium bromide/poly(dA)/poly(dT) as a function of the NaCl concentration is shown. Enhancement of the fluorescence intensity I_F was observed at NaCl concentrations higher than 5 mM, before the intensity gradually decreased with increasing NaCl concentration. This decrease in fluorescence intensity observed at high NaCl concentration is due to the decrease in the binding constant between ethidium bromide and poly(dA·dT), as shown by *Maiti* and co-workers [28]. All together, these findings reveal that poly(dA) and poly(dT) form the duplex at NaCl concentrations higher than *ca.* 5 mM. Under the same conditions, the CD spectra showed a synchronized change, which prompted us to conclude that CD spectroscopy is well-suited to follow duplex formation between poly(dA) and poly(dT).

Takeover Reaction of poly(dA) from the s-SPG Complex to poly(dT). These experiments were performed at a NaCl concentration of 150 mM, which is close to physiological conditions. In *Fig. 3, a*, two possible scenarios are shown schematically when poly(dT) is added to poly(dA·2s-SPG): *1*) takeover reaction of the poly(dA) chain from the s-SPG complex to poly(dT) under poly(dA·dT) duplex formation, or

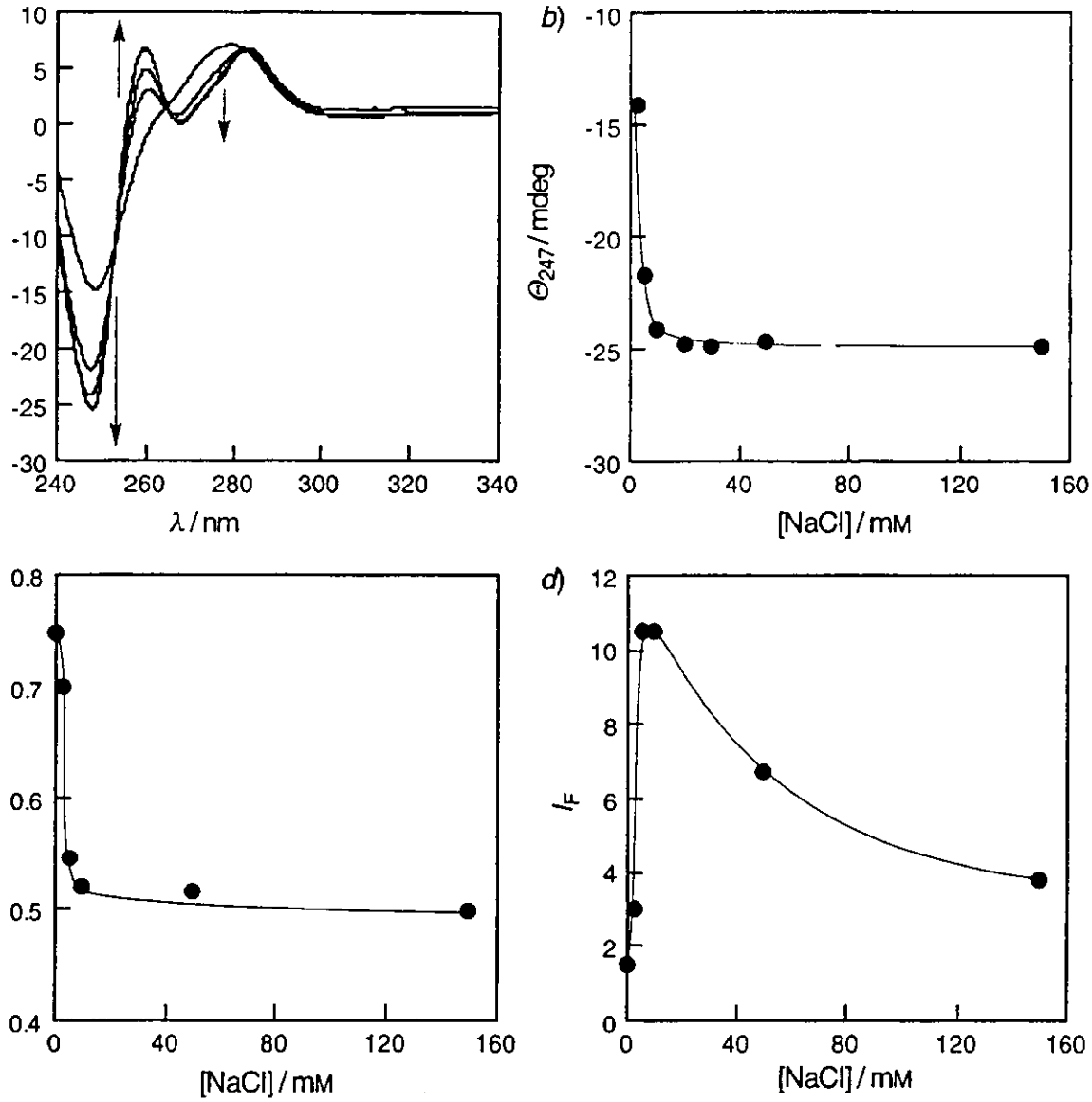

Fig. 2. *Influence of NaCl concentration on the spectral properties of mixtures of poly(dA) and poly(dT).* a) *CD Spectra* (3–150 mM NaCl); b) *plot of the CD ellipticity at 247 nm* (Θ_{247}) vs. *NaCl concentration*; c) UV/VIS absorbance (Abs) *at 260 nm*; d) *relative fluorescence intensity* (I_F) *at an emission wavelength of 590 nm.* Conditions: [Poly(dA)] = [poly(dT)] = 37 μM/repeating unit; T = 37°.

II) retention of the triple-helical complex despite addition of poly(dT). In the first case, the CD spectrum of poly(dA·2s-SPG) should change to that of poly(dA·dT) (solid line in *Fig. 3, b*), whereas, in the second case, a spectral change from poly(dA·2s-SPG) to the averaged CD spectrum of the poly(dA·2s-SPG)/poly(dT) mixture (dotted line in *Fig. 3, b*), is expected.

The experimentally observed CD spectral changes upon addition of poly(dT) to poly(dA·2s-SPG) at 37° are shown in *Fig. 3, c*. Before the addition of poly(dT) (broken lines), the CD spectrum was identical with that for poly(dA·2s-SPG) [18], confirming that the complexation was complete. Immediately after the addition of poly(dT), the

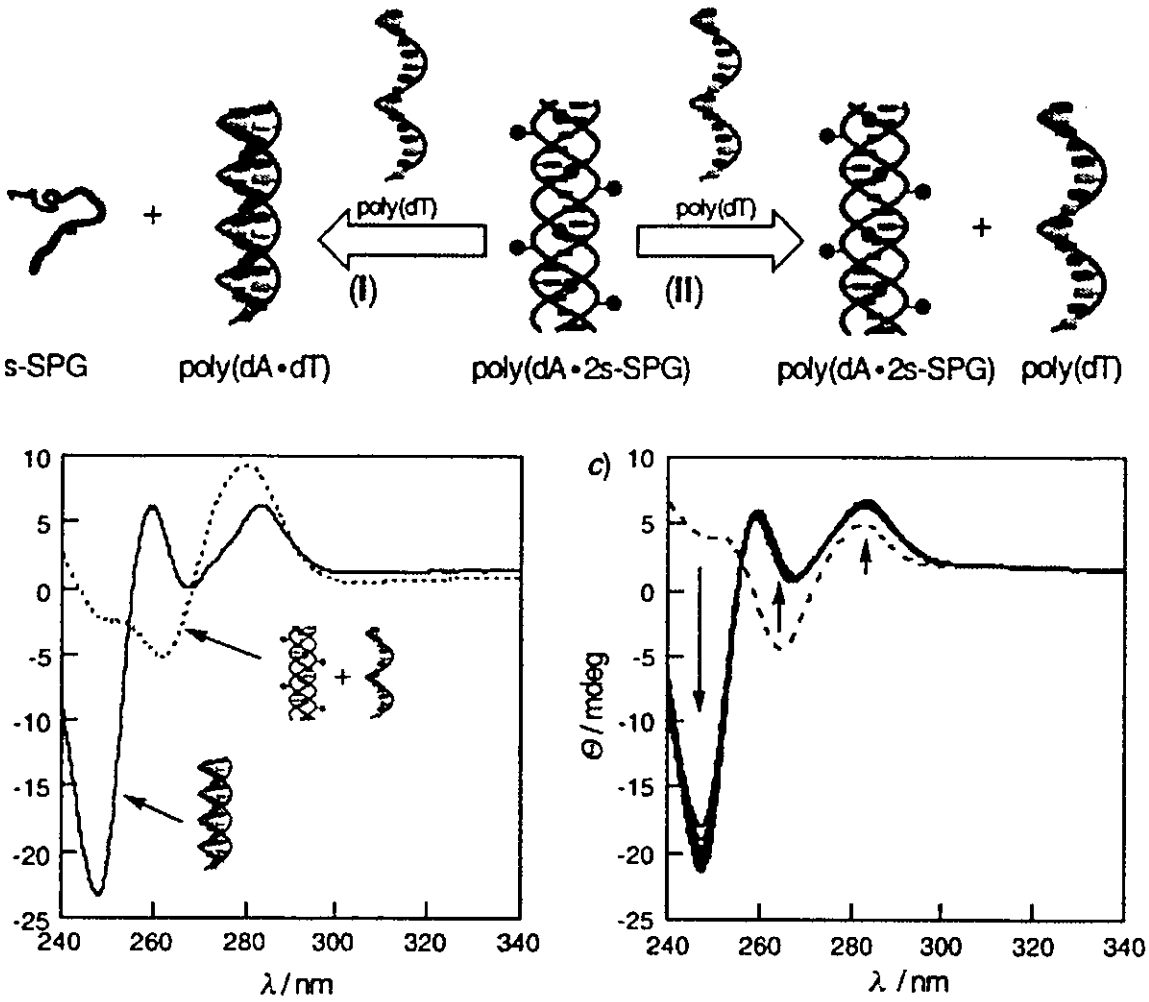

Fig. 3. a) *Schematic illustration of two possible scenarios upon addition of poly(dT) as the complementary strand to poly(dA)·2s-SPG.* b) *CD Spectrum of poly(dA·dT)* (solid line) *and calculated CD spectrum of the mixture of poly(dA)·2s-SPG and poly(dT)* (dotted line). c) *Time-dependent CD spectral changes after addition of poly(dT) to poly(dA)·2s-SPG.* Broken line: before addition of poly(dT); solid lines: CD spectra taken in 10-min intervals after addition of poly(dT). Conditions: [poly(dA)] = [poly(dT)] = 37 μM/repeating unit; [s-SPG] = 25 μM/repeating unit.

spectrum changed drastically, indicating formation of poly(dA·dT). The takeover reaction occured so quickly that the initial change could not be followed (*ca.* 75% of poly(dT) had been hybridized with poly(dA) within 1 min).

Next, we evaluated salt effects. In *Fig. 4*, the change in CD ellipticity, $-\Delta\Theta_{247}$, is plotted against reaction time for various NaCl concentrations. Here, $-\Theta_{247}$ is defined by subtracting the calculated CD ellipticity of the mixture of poly(dA·2s-SPG) and poly(dT) proper from that at a given reaction time. At 3-mM NaCl concentration, the hybridization between poly(dA) and poly(dT) cannot take place owing to the large repulsion between the phosphate anions, so that there was no increment in $-\Delta CD_{247}$, in contrast to higher NaCl concentrations. Judging from these experiments, it is obvious that the takeover reaction commonly takes place whenever poly(dA) forms a duplex with poly(dT).